Satellite Attitude from a Raven Class Telescope

Daron Nishimoto
David Archambeault
Pacific Defense Solutions, LLC

David Gerwe
The Boeing Company

Paul Kervin
Air Force Research Laboratory, RDSM

Abstract

Photometric signatures of satellites collected from small aperture optical systems have the potential of providing valuable satellite information including operational status and attitude. Low cost, small aperture systems provide the capability to be transportable and therefore used in a wide variety of deployment scenarios. This research describes the benefits of prior knowledge of the satellite under consideration including general size, shape and typical material properties. By constraining the problem to a discrete set of satellite attitudes, curve matching algorithms can then be used to compare the measured photometric signature against those in the forward modeled database. TASAT simulations were used to create a database of forward modeled photometric signatures. In this paper, we explore two curve matching techniques. The first method was Kendall's Tau which compares the shapes of two curves. The second method was the Spectral Angle Mapper (SAM) which measures the similarity of two curves that have been processed to remove their mean values. The key findings of this study are the generation of a database of signatures to which a measured signal can be compared to extract attitude information about the satellite during a specific pass.

1. Introduction

Photometry is the measurement of an object's apparent brightness, usually measured within a specific calibrated wavelength band. A photometric signature is produced by several measurements of the object's brightness over a known time period. For this study, the time period is the duration of the satellite pass from horizon to horizon. For geometric considerations, when the satellite attitude is in a ground-pointing orientation above an area of interest, the satellite's surface orientations with respect to the optical sensor and the source of illumination (e.g. the sun) varies creating increasing or decreasing intensities, and thus produces a photometric signature that varies as a function of the attitude of the satellite. The objective of this feasibility study was to determine if the attitude of a particular satellite produces a unique photometric signature that could be matched to a database of previously generated satellite signature models to within 2° of a satellite attitude change and a 90% classification accuracy.

The findings of this paper provide insight into the shape and attitude recovery problem in that there are many sources of variation in the signatures. The first problem being that space materials are not always accurate on the models used for the simulation of the database of signatures. This is important when trying to simulate satellites that are not owned or operated by cooperative entities. The second source of signal degradation is the calibration accuracy of the atmospheric transmission. This value is measured on the sensor by the use of calibration stars, and is desired to be less than 5% for good radiometry, and 1% for excellent radiometry. Lastly, every possible position of the satellite cannot be simulated in a timely fashion, and thus a good portion of the database should reflect orientations that are of value to the observing location for signature comparison. This provides a limiting number of solutions and highly constrains the problem down to a specific number of signatures. Results show that with moderate calibration errors, of ± 20%, the Spectral Angle Mapper (SAM) technique matches correctly to the database with a 90% success rate for a cylindrical type of satellite in a high-elevation pass.

Report Documentation Page

Form Approved
OMB No. 0704-0188

1. REPORT DATE	2. REPORT TYPE	3. DATES COVERED
SEP 2010		**00-00-2010 to 00-00-2010**

4. TITLE AND SUBTITLE	5a. CONTRACT NUMBER
Satellite Attitude from a Raven Class Telescope	5b. GRANT NUMBER
	5c. PROGRAM ELEMENT NUMBER
6. AUTHOR(S)	5d. PROJECT NUMBER
	5e. TASK NUMBER
	5f. WORK UNIT NUMBER
7. PERFORMING ORGANIZATION NAME(S) AND ADDRESS(ES)	8. PERFORMING ORGANIZATION REPORT NUMBER
Air Force Research Laboratory,AFRL/RDSM,Kihei,HI,96753	
9. SPONSORING/MONITORING AGENCY NAME(S) AND ADDRESS(ES)	10. SPONSOR/MONITOR'S ACRONYM(S)
	11. SPONSOR/MONITOR'S REPORT NUMBER(S)

12. DISTRIBUTION/AVAILABILITY STATEMENT

Approved for public release; distribution unlimited

13. SUPPLEMENTARY NOTES

2010 Advanced Maui Optical and Space Surveillance Technologies Conference, 14-17 Sep, Maui, HI.

14. ABSTRACT

Photometric signatures of satellites collected from small aperture optical systems have the potential of providing valuable satellite information including operational status and attitude. Low cost, small aperture systems provide the capability to be transportable and therefore used in a wide variety of deployment scenarios. This research describes the benefits of prior knowledge of the satellite under consideration including general size, shape and typical material properties. By constraining the problem to a discrete set of satellite attitudes, curve matching algorithms can then be used to compare the measured photometric signature against those in the forward modeled database. TASAT simulations were used to create a database of forward modeled photometric signatures. In this paper, we explore two curve matching techniques. The first method was Kendall's Tau which compares the shapes of two curves. The second method was the Spectral Angle Mapper (SAM) which measures the similarity of two curves that have been processed to remove their mean values. The key findings of this study are the generation of a database of signatures to which a measured signal can be compared to extract attitude information about the satellite during a specific pass.

15. SUBJECT TERMS

16. SECURITY CLASSIFICATION OF:			17. LIMITATION OF ABSTRACT	18. NUMBER OF PAGES	19a. NAME OF RESPONSIBLE PERSON
a. REPORT	b. ABSTRACT	c. THIS PAGE			
unclassified	**unclassified**	**unclassified**	**Same as Report (SAR)**	**10**	

The remainder of this paper is organized as follows. Section 2 describes the end-to-end modeling and simulation setup, Section 3 deals with the signature generation process with TASAT and Raven class telescopes, Section 4 discusses the curve matching results to the database and Section 5 discusses the conclusions.

2. End-to-End Modeling and Simulation

Fig. 1 illustrates the end-to-end modeling and simulation environment used to test and evaluate the two curve matching algorithms. AFRL's *j*Track[1] software tool computes a set of possible satellite orientations in 6 Degrees of Freedom (6DoF), commensurate satellite attitude geometries or orientation, and computed Earth tracks. The attitude geometries and Earth tracks are stored in two separate caches. The *Earth Track Cache* is maintained until the signature matching process has completed. The information stored in the satellite *Geometry Cache* is used as input into the *Time-domain Analysis and Simulation for Advanced Tracking* (TASAT)[2] software, which then produces photometric signatures for each of the potential satellite orientations, from the *Geometry Cache*, that are stored in the *Photometric Signature Cache*.

For this small aperture study, a Raven class telescope was modeled as a Celestron 11", Apogee Alta U47 (1024 x 1024, 13µm pixels) stationed at the Remote Maui Experiment (RME) located in Kihei, Maui. In the simulation, a Raven class sensor generates a raw scene-simulated satellite photometric curve. The *Photometric Signature Atmospheric Effect Compensator* algorithm receives and compensates the signature for atmospheric absorption and scattering effects. For the base model, the only source of noise is Additive White Gaussian Noise (AWGN) that degrades the signature as a read noise term. The *Photometric Signature* Comparator algorithm then compares the calibrated photometric signature to the *Photometric Signature Cache* and returns the best match within the 2° angle-estimation accuracy requirement. It should be noted that observations of calibration stars in conjunction with each pass is necessary to properly calibrate the measured photometric signatures. The atmospheric degradation is removed by division of the transmission curve from the measured signature to produce an exo-atmospheric intensity. This exo-atmospheric intensity signature is then compared to the simulated signatures via the *Photometric Signature Comparator*. The results from the signature comparator feed directly into the ground track solutions provided in the *Earth Track Cache* showing near real-time orientation results.

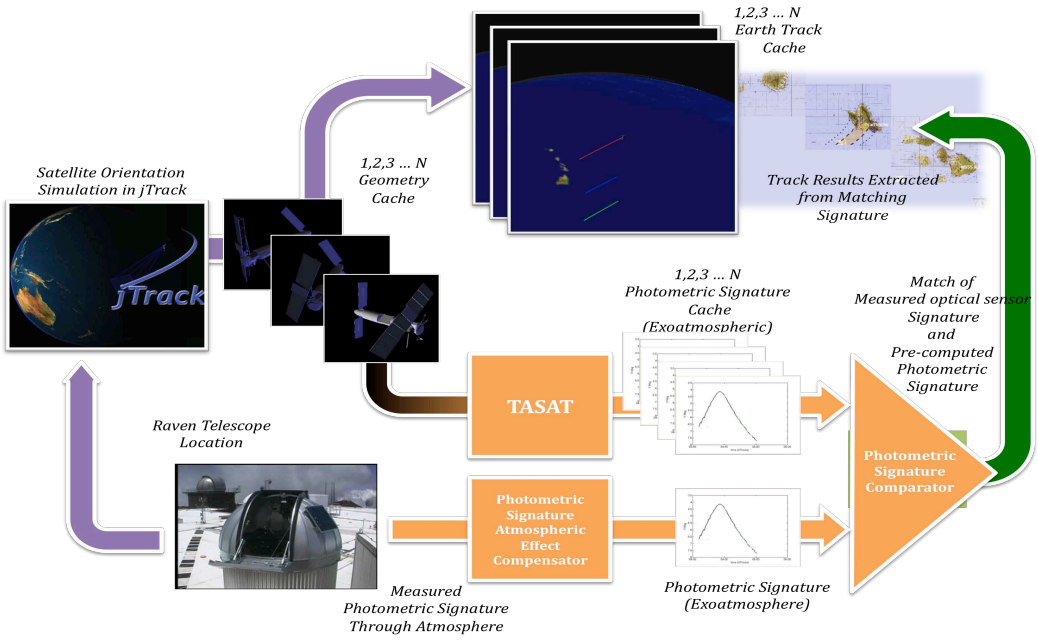

Figure 1. Processing Flow Simulation for Determining Earth Tracks

Two distinct 3-D satellite bus type models were built in the New Solid Model (NSM) format with the Solid Modeling Tool (SMT) to test the photometric signature matching algorithms. The models consist of a body-pointing ***cylindrical*** satellite system and a body-pointing ***cubic*** satellite system. These features are representative of many earth-observing satellites. Fig. 2, shows a cylindrical satellite bus representing a telescope imaging system, which

provides a unique signature for specific phase angles. Fig. 3, shows a cubic satellite bus representing a dual imaging bus with protruding shade cones or antennas. The cubic satellite bus presents a more difficult photometric signature matching problem than the cylindrical imager due to the symmetry of the satellite.

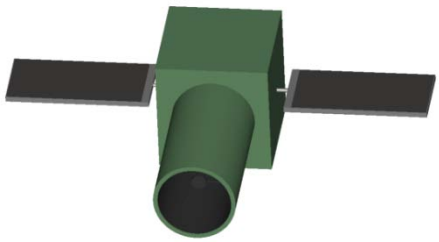

Figure 2. Cylinder Satellite Model

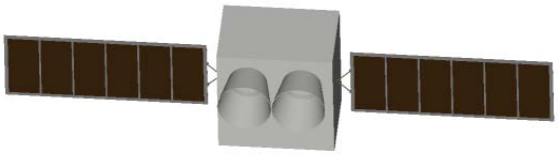

Figure 3. Cube Satellite Model

First, a satellite orbit is generated simulating an earth-observing pass for a particular area of interest on the ground. Using the models in Fig. 2 and 3, built with the +Z-axis in the payload direction, the *j*Sim software tool computes the satellite orbit based on two-line element sets (TLE). After the orbit is computed, the location of the specific area of interest is used to generate the satellite body-point angles required to image that particular area. This rotation value, estimated as a cross-track roll angle, is used to generate the Geometry Cache required to populate the Photometric Signature Cache. The +Z-axis in the body frame of the satellite is rotated away from the nadir vector to generate the roll values, with one or more of these rotations pointing at the ground observer. The cross-track values are a simplification to the general problem of using in-track (pitch) and cross-track (roll), decreasing the amount of angles required for simulation. The remainder of this report will focus on the results from the Cylinder Satellite model only.

Solid Modeling Tool (SMT) Reflectance Curves

The materials that were selected from the SMT material database in developing the satellite models were Aluminized Kapton, Multi-layer Insulation (MLI), Solar Stack and Blue Silicon Solar Cells. The material reflectance curves for the Cylinder and Cube Satellites are displayed in the figures below. The reflectance values are provided by the Satellite Assessment Center (SatAC) in a file distributed with both TASAT and SMT called the Materials Database. Fig. 4 shows the reflectance of Aluminized Kapton that is used as the outer material for the main body of Cylinder Sat. Fig. 5 displays the reflectance curve for the solar stack material of the Cylinder Sat. Fig. 6 displays the reflectance curve for the MLI that covers the outer layer of Cube Sat. Lastly, Fig. 7 shows the solar panel reflectance of Cube Sat that consisted of Blue Silicon Solar Cells. It should be noted that the wavelengths of the simulations for this project were conducted in the 700 nm – 1200 nm, or I-Band, range.

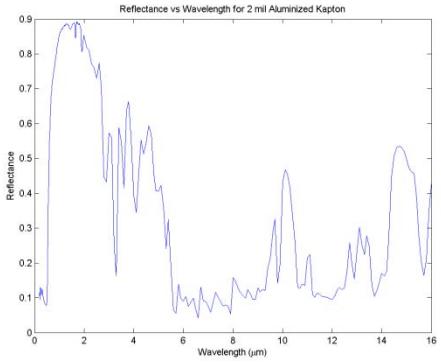

Figure 4. Reflectance function of Cylinder Sat surface material, 2 mm Aluminized Kapton.

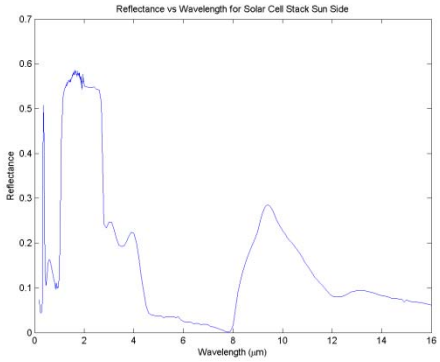

Figure 5. Reflectance function of Cylinder Sat solar panel material, Solar Stack sun side.

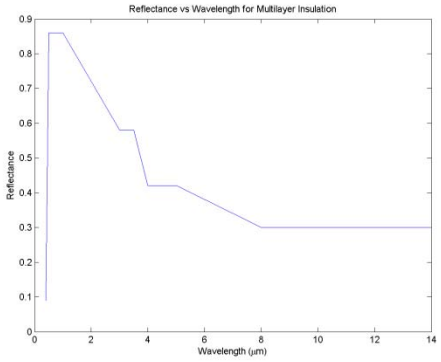

Figure 6. Reflectance function of Cube Sat surface material, Multi-layer Insulation (MLI)

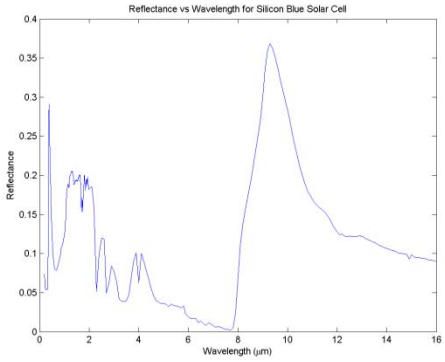

Figure 7. Reflectance function of Cube Sat solar panel material, Blue Silicon Solar Cell.

It should be noted that the wavelengths of the simulations for this project were conducted in the 780 nm – 1200 nm, or I-Band, range. When combined with the Silicon response curves of the camera system the overall waveband response becomes 780 nm – 980 nm. Total reflectance curves of the entire system are not possible to generate due to the complex relationship between the components. To overcome this complexity, TASAT handles the individual ray tracing for each surface and each pixel with the ability to add multiple reflections when generating the photometric light curves.

3. Raven-class Photometric Signature Simulated with TASAT

AFRL's Time-domain Analysis and Simulation (TASAT) software was used to simulate the calibrated photometric signatures which would result from data collected from a Raven-class telescope. TASAT builds a detailed optical tracking scenario given multiple optical and satellite inputs, and determines the position and orientation of a satellite in the Earth Centered Inertial (ECI) reference frame. Based on the inputs, a ray-tracing algorithm within TASAT computes the solar reflectance of the satellite from a light source (Sun) to the Raven optical sensor. There were constraints placed on the orbit of the satellite and the observing location. All passes culminated over the observing location at an elevation greater than 45° and were in a terminator period to eliminate sky foreground complications

Atmospheric Errors

Based on the assumption that the aperture photometry technique accounts for all sensor calibration characteristics such as removing read noise and dark currents, the atmosphere becomes the largest source of errors. To simulate this source of errors, the photometric signatures that are generated are perturbed by a nominal atmospheric extinction of 0.17 and then corrected with a measured extinction value between 0.10 and 0.24, or alternatively a maximum of 40% error in atmospheric calibration. The values that are less than the nominal value of 0.17 are underestimating the atmospheric extinction and thus are not correcting the measured signatures enough, while the values greater than 0.17 are overestimating the extinction of the atmosphere and generate larger values than what should be measured. The difference in the signature when multiplied by the nominal transmission curve and then divided by the measured transmission curve are the definition of the atmospheric calibration errors. This horseshoe shape of the transmission curve versus elevation of the satellite provides larger errors at the start and end of a pass relative to the nominal signal strength while causing a scalar offset in the middle parts of the pass.

Photometric Signature Matching

Photometric signature matching algorithms were applied to the measured photometric signature to match to the database of forward modeled photometric signatures in the Photometric Signature Cache. The two photometric signature matching algorithms that were selected for this study are named TAU, for an implementation of Kendall's Tau[3], and the Spectral Angle Mapper[4], or SAM. The TAU algorithm uses Kendall's Tau as a measure of the likeness of two shapes using a two-dimensional difference surface and a correlation type metric. The SAM method is the spectral angle mapper, and uses an *N*-dimensional dot product, and relies on the mathematics of the dot product having zero angle difference for two parallel vectors.

Kendall's Tau is a measure of the similarity between two different shapes, or in this case, two different photometric signatures. This method requires that we form what is known as a derivative surface by piecewise comparing of each simulated photometric signature with itself. A similar surface is then created using the measured signal. Once the 2D surfaces are retrieved from the 1D signals, we compare the number of points in the two surfaces that are the same and different. The photometric signature that maximizes Kendall's Tau, as this is value is a correlation metric, is the best estimate. The valid range of values for the Kendall's Tau are [-1,1] with 1 being an exact match and -1 being an exact mirror-mismatch. Because the method relies on comparisons of slopes, the similarity of shapes of photometric signatures is more important than absolute values.

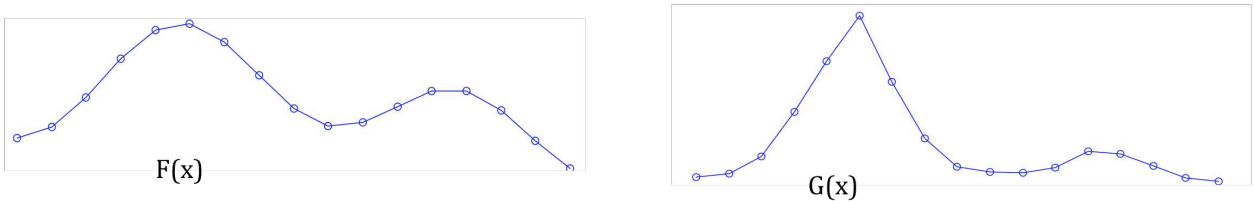

Figure. 8. Curves used to demonstrate Kendall's Tau method of curve matching in which G(x) is almost a monotone transformation of F(x).

Consider the two sample photometric signatures in Fig. 8. For example, photometric signature F(x) represents the measured photometric signature from an optical sensor, while photometric signature G(x) represents one of the photometric signatures from our forward-modeled Photometric Signature Cache database. In Fig. 8, G(x')-G(x) has the same sign as F(x')-F(x) for almost all pairs (x, x'). While there are certainly differences, they do have roughly similar shapes. We now discuss criteria by which formal definitions of similarity are established.

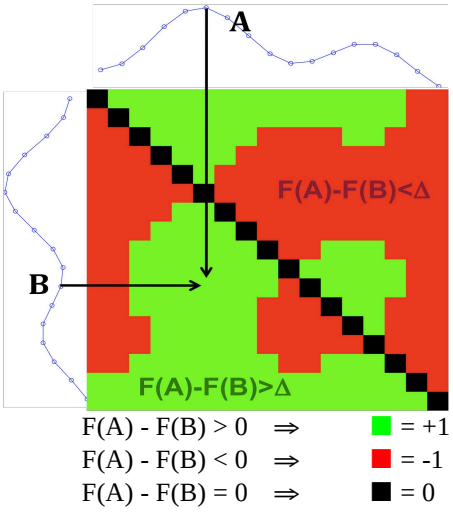

Figure. 9. Construction of the two-dimensional difference function.

In the Kendall's Tau method, we examine how differences in pairs of points on the photometric signatures compare. Fig. 9 shows the results of comparing a function F at two points A and B by subtraction as F(A)-F(B). When A=B, we are comparing the function at the same point, so the value is zero, and thus the diagonal along all surfaces will be zero. The Kendall's Tau method depends only on the fact that there may be a difference in the values at the two points, and not on the magnitude of the difference. Therefore, if F(A)>F(B) we assign the value +1 at the pair (A,B). If F(A)<F(B) then we assign -1. This results in a two-dimensional map as shown in Fig. 9 where green squares indicate a positive difference, red squares indicate a negative difference and black squares represent a zero location.

Fig. 10 shows that the difference map for G(x) is nearly the same as for F(x), displaying many similar traits functionally. To determine how similar the two curves are, we need to count the number of similar and dissimilar points exist. Thus, where both maps have the same sign, we say that there is a concordance, and denote that count by

C. Where the two maps have different signs, there is a discordance and that count is denoted by D. Therefore, we have just counted the number of matching and mismatching points in the two surfaces of F(x) and G(x) into the values of C and D. The difference C-D is then a measure of how close the two maps are to each other. We can normalize that quantity by dividing by the number of pairs, which can be formed from our *N* samples.

In Fig.10, G(A)-G(B) has the same sign as F(A)-F(B) for almost all pairs A,B. This is an indication that the two photometric signatures are very similar. To determine how similar, the Kendall's Tau value is computed by using the definitions of C (matching pairs), D (mismatched pairs) and *n* (total number of pair) in (1).

$$\tau = \frac{C - D}{\frac{n}{2}(n-1)} \tag{1}$$

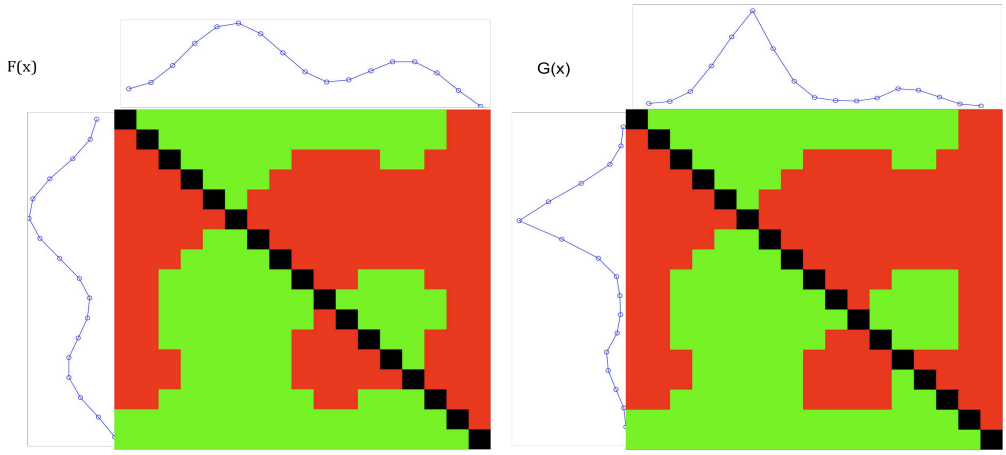

Fig. 10. The second signal is almost a monotone transformation of the first.

The second algorithm is the Spectral Angle Mapper (SAM). The origins of the SAM metric in [5] are derived from remote sensing data used to compare regions of space based images taken of the ground. The SAM metric, in (1) becomes an angle in an *N*-dimensional space between two *N*-dimensional vectors. The two vectors are the incoming data stream of the measured signature and one of the simulated data, or database signature, streams. Formally, denoting the vectors as $I_m(t_1,t_2,t_3, \ldots t_N)$ for the measured data and $I_s(t_1,t_2,t_3, \ldots t_N)$ for the simulated data set, we form the dot product of the two vectors, as shown in (2).

$$I_m \circ I_s = |I_m||I_s| \cos\theta \tag{2}$$

Then, based on the values in (2), θ is the spectral angle. The smaller the value of θ, the more alike the two vectors, however, the specific constraint on the timing of the sequences apply. If the vectors are not put on the same time scales, and synchronized, the results may be skewed. For this project, all photometric signatures are perfectly aligned in time, and constitute a continuous data set. In other words, there are no breaks in the data stream from clouds, equipment malfunctions, or operator errors.

Generation of Earth Track/Photometric Signature Cache

MATLAB was used as an interface to the *j*Sim libraries, including orbit propagation, Earth Track determination, and satellite orientation methods. The inputs to *j*Sim include the satellite TLE, time of interest, an asset location (latitude/longitude/altitude), and Raven sensor location. *j*Sim uses the standard Air Force SGP4 propagator to compute the position of the satellite during the time of interest to compute the photometric signature collection opportunities of the satellite.

The combined software tool calculates the satellite orientation required to image the asset location. The software then computes the orientation required to image the asset with only a roll maneuver. This keeps the number of angles for simulation to a minimum and matches the operational capabilities of many Earth Imaging satellites. The cross-track roll angle is found at the nearest ½ second around culmination. This distinct orientation angle, or threat angle, is then used as the basis for signature generation to determine if an asset or location has been imaged.

To minimize the simulation processing time for this study, a smaller set of different rotation angles are computed that encompass the threat angle and include the unique nadir down orientation. The simulation data set includes the rotation angles spanning the threat angle in ten 2° steps for a total of 21 unique rotation angles, or +/- 18° of coverage around the threat angle. The nadir down orientation is included specifically as a common satellite cruise mode and provides a signature that could indicate a satellite is currently not performing an imaging mission.

4. Results

Photometric Signature Matching Performance

The simulations performed for this performance analysis consisted of two different satellite bus structures; two different elevation passes with two dramatically different lighting conditions, or phase angles. In addition, over 21 different levels of atmospheric calibration errors were applied to degrade the signatures before comparison to provide a number of samples for comparison. The performance of the algorithms degrades as the amount of calibration error increases, and can be seen in the following figures. Providing each of the possible signatures as truth for each calibration error value produced these figures. Counting the number of times each orientation was correctly estimated and when each pose was incorrectly estimated generates the success rates. This process was done again by adding the equivalent of read-noise in the form of zero-mean data Gaussian data. This small amount of noise on the large values of the signatures produces a different result in the comparison algorithms based on the type of satellite being observed.

The performance of the signature matching algorithms for a high elevation pass for the Cylinder Sat model is shown in Fig.11 and Fig. 12. The data in Fig. 11 shows the performance for an exact match of the signatures, while Fig. 12 contains the performance for a ±2° approximation window around the exact match. The red curve depicts the Spectral Angle Mapper (SAM), the blue curve depicts the Kendall's Tau method, and the green curve is an RMS method used to show a baseline comparison. The results show that SAM is the best matching algorithm for the Cylinder Sat for both the precise orientations and approximate orientations. But, as the calibration error increases from either over-estimation or under-estimation, of the atmospheric transmission, all the comparison algorithms fall off in the number of correct satellite orientation estimations, with only the photometric signatures with strong features being correctly estimated. The strong features that occur in the Cylinder Sat case are glints off the imaging tube of the satellite. Also shown in the figures are the curves that do not have read-out noise degradation and those that had a read-out component comprised of zero-mean Gaussian noise a standard deviation of 25 W/sr. The performance of the noise degraded curves is shown in dashed lines while the noiseless curves are solid.

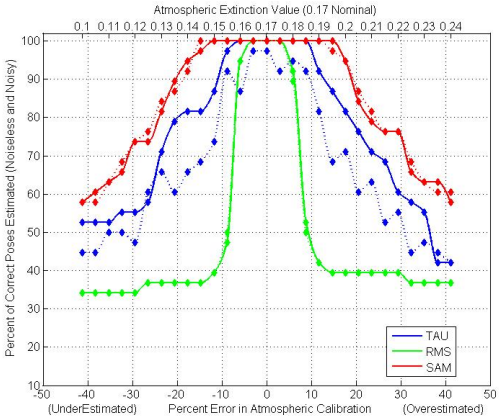

Figure 11. Cylinder Sat, High Elevation, Photometric Signature matching Performance Curves (exact)

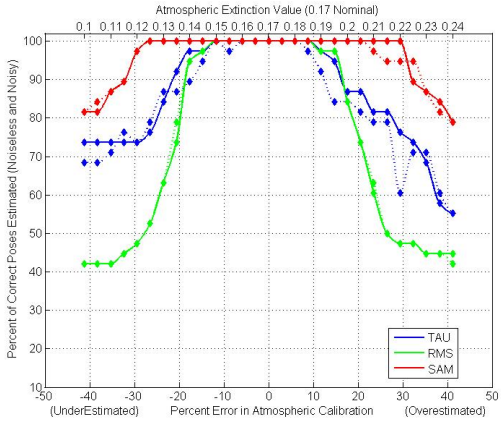

Figure 12. Cylinder Sat, High Elevation, Photometric Signature matching Performance Curves (approximate)

When the pass geometry is moved from a 'high elevation' to a 'low elevation' situation the results of the curve matching changes. The results shown in Fig. 13 provide the exact solution match for the Cylindrical Satellite that culminates at an elevation of 53° from the observing location. This is in contrast to the 84° elevation of the high-elevation situation previously described. The exact solution performance curves show good performance out to ±40% calibration errors. The performance shows that Kendall's Tau is now the better metric when compared to SAM for this instance. The SAM performance drops more rapidly on the positive side of the calibration errors, while Kendall's Tau is nearly always above 90% successful. On the negative side, or underestimated errors, SAM performs better against itself, but Kendall's Tau remains better with a higher percentage of correct estimates. When the conditions for correctness are loosened to the ±2° in any one angle, Kendall's Tau is nearly 100% correct for this type of satellite in this geometric configuration, and can be seen in Fig. 14. SAM has nearly identical performance in the exact and approximate solution configurations with the exception of a few percentage points. Further investigation is required to determine a cause for this behavior, and if the signature database is a source for the similarity, or if there is something inherent in the curve matching algorithm.

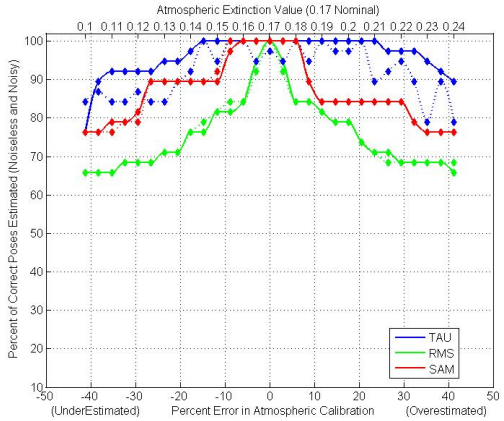

Figure 13. Cylinder Sat-Low Elevation, Photometric Signature matching Performance Curves (exact)

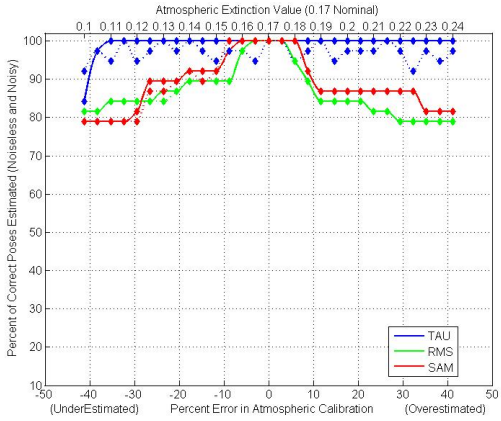

Figure 14. Cylinder Sat-Low Elevation, Photometric Signature matching Performance Curves (approximate)

Photometric Signature Matching Summary

For Cylinder Sat, in a high elevation pass (greater than 65°), SAM provided better performance. The results for the Cube Sat match that of the Cylinder Sat, and is the main reason those results are omitted in this report. In lower elevation passes (below 65° and greater than 50°), Kendall's Tau provided better performance for the Cylinder and Cube satellites. Because of the different geometric configurations providing different results for each method a weighting could be applied to the algorithms based on elevation, and satellite type if known, to determine the algorithm best suited to the observing situation. These results provide a solid foundation for the Monte Carlo simulation testing utilizing the end-to-end environment discussed in the results section below.

Generalized Classification Accuracy Testing

To test and verify the classification accuracy a test was developed where an individual test is defined by measuring the performance of the algorithm for a representative set of satellite passes over a 30-day period that a Raven class optical sensor would observe. If the single forward modeled photometric signature (FMPS) solution was correctly matched, then the individual pass will be said to be "Correctly Classified". If an incorrect FMPS was matched, the pass will be labeled as "Mis-classified." The aggregate Classification Accuracy accumulated over the simulated 30-day period will be used to determine if the test passed or failed. The success criteria of this testing is set at a classification accuracy of 90% previously stated.

Over a 31 day period, six generalized satellites were simulated from 1 December 2009 00:00:00 to 31 December 2009 23:59:59. This resulted in 94 passes fitting the parameters of the pass finder. The parameters in this case were that the pass needed to culminate over the observing site at least 45 degrees in elevation and be solar illuminated while the observing site was dark, or terminator conditions. The sensor location was set to be at the RME in Kihei,

Maui. To perform the test each satellite pass was given four signatures to be compared. These signatures consisted of: the satellite observing the observer, a signature that was within two degrees of the observer, the nadir signature and a randomly chosen signature that was not part of the previous three photometric signatures based on the angles described earlier. Together these four signatures provide different test cases for the photometric signature matching algorithm and the satellite orientation estimation accuracy.

For each test case the satellite pass information was read into a software suite that contains the algorithms. The software suite is responsible for generating the TASAT signatures, or the forward modeled photometric signatures (FMPS), and the Kendall's Tau surface maps, and feeds directly into the signature matching algorithms. To thoroughly test the robustness of the algorithms, each individual test on each signature used a random calibration error value in the bounds of [-20, 20] percent. In addition to the calibration error, zero-mean random Gaussian noise was also added to the measured photometric signature (MPS). After degradation of the MPS, curve matching was performed for each of the four photometric signatures for each satellite pass, or simulation. When performed over the 94 different satellite passes there were a total of 376 different photometric signature matches performed. This test was performed 50 times for a total of 18,800 realizations of a MPS to be compared to each simulated FMPS. The results of these tests are summarized in Table 1. The Classification Accuracy metric is shown below in (3) and is displayed in the last column of Table 1.

$$ClassificationAccuracy = 100 - \frac{\sum(IncorrectSolutions + MultipleSolutions + NoSolutions)}{TotalClassifcationsAttempted} \quad (3)$$

Table 1. Testing Results for Classification Accuracy of software suite with curve matching algorithms.

Description of Test	Number Correct	Classification Accuracy
Completely Correct Satellite orientation Estimates -Both Methods Agree	17145	91.2%
Correctly Estimated by TAU Method -TAU Correct, SAM Incorrect	17220	91.6%
Correctly Estimated by SAM Method -SAM Correct, TAU Incorrect	18668	99.3%
Correctly Estimated by Either Method -SAM Correct or TAU Correct	18762	99.8%

To present the data in another way, a bar graph depicting the percentage of satellite orientations correctly estimated is shown in Figure 15. Overlaid on the bar chart are two other plots showing the actual number of satellite orientations incorrectly estimated, for each 376 different comparisons, and the number of incorrectly estimated satellite orientations when neither algorithm got the solution correct. Drawn across the top of the chart is the success rate of 90%. Many of the different tests are above this threshold, but a few are not. Overall, the software and the algorithms were able to correctly estimate 91.2% of all the satellite orientations when both the Kendall's Tau and Spectral Angle Mapper agreed on the satellite orientation.

Since there were never "No Solutions", as the software always chooses a solution, then the problem reverts to when the two methods disagree on the estimated satellite orientation. If we look at the data when there were "Multiple Solutions" chosen by the software, it is important to see how many of those were actually correctly estimated by one of the algorithms. The data shown in Figure 16 is the number of correctly estimated satellite orientations by either one of the algorithms and the number of incorrect solutions is overlaid. By using this method, the percent of correctly estimated satellite orientations jumps to 99% correct.

Classification Accuracy Summary

In summary, the correct satellite orientation was estimated correctly greater than 90% of the time, which was the goal of this project. A satellite orientation is correctly estimated when both algorithms agree on the satellite orientation. A satellite orientation is marked as "Multiple Solutions" when the two algorithms disagree on the

satellite orientation. When the algorithms did disagree on the satellite orientation estimate, 99.8% of the time one of the two algorithms got the correct solution. This means that there was only 0.2%, or 36 passes, incorrectly classified out of 18,800.

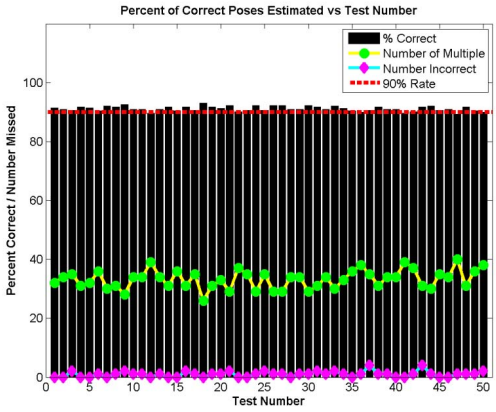

Figure 15. Results for the Classification Accuracy testing when both methods agree on satellite orientation estimate.

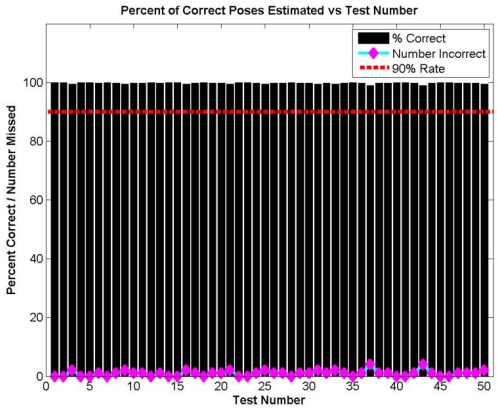

Figure 16. Results for the Classification Accuracy testing when either of the two algorithms correctly estimates satellite orientation within two degrees.

5. Conclusion

This feasibility study focused on the use of forward modeled photometric signatures and two curve matching techniques to determine a best fit solution to a measured signature of a satellite. The biggest assumption made is that the photometric technique used on the sensor accounts for the calibration errors in the system, leaving the atmospheric transmission as the only source of corruption. This corruption is introduced as a erroneous estimate in the extinction coefficient off of a nominal value of 0.17. At less than ±10% atmospheric calibration errors the SAM method is able to correctly identify greater than 95% of passes for a cylindrical satellite during a high elevation pass as seen in Figure 11. By lifting the pose estimate restricts to 2° in one angle, the ability of SAM to correctly estimate poses with 95% accuracy expands to ±30% atmospheric calibration errors. If the satellite is in a lower elevation geometry, the Kendall's Tau method is then the best estimator for poses. This is shown in Figure 13 and the Kendall's Tau correctly estimates poses 95% of the time with calibration errors up to ±20%. When using the two methods in combination with each other over a Monte Carlo simulation of 18,800 different signatures, the post was correctly estimated 99.8% of the time. Kendall's Tau and the Spectral Angle Mapper provide a feasible way of comparing measured signatures to forward modeled photometric signatures with a high degree of accuracy, given that the forward model is accurate.

6. References

[1] Roggemann, M.C., Hamada, K., et. al., "Three-Dimensional Imaging and Satellite Attitude Estimation Using Pulse Laser Illumination and a Remote Ultra-Low Light Imaging (RULLI) Sensor for Space Situational Awareness (SSA)", AMOS Conference Proceedings, 2008.

[2] TASAT Software Users Manual, TASC (formerly Northrop Grumman Information Technology), June 12, 2008.

[3] Kendall, M., "A New Measure of Rank Correlation", Biometrika (1938), 30(1-2), pp 81-93.

[4] Kruse, F. A., Lefkoff, A. B., et. al, "The Spectral Image Processing System (SIPS) – Interactive Visualization and Analysis of Image Spectrometer Data", J. Remote Sens (44), pp. 145-163, 1993.